

CHAPTER 8

Genetic, phenotypic and biochemical characterization of *ppc* genomic integrant *Pseudomonas P4*

"Every time a man puts a new idea across he finds ten men who thought of it before he did-but they only thought of it."

-Anonymous

8.1: INTRODUCTION

Genetic modifications in pseudomonads described so far involved overexpression of selected genes from a strong promoter on multi-copy broad host range plasmids. Effect of these modifications comprise of number and promoter properties of the genes in the transformants along with metabolic load arising due to the maintenance of additional plasmid coupled with expression of antibiotic resistance genes. High level expression of foreign gene(s) from a strong promoter on high-copy number expression vectors often exerts metabolic burden on the cell. Such a metabolic load is generally attributed to increased precursor and energy demands for plasmid replication and plasmid-encoded mRNA synthesis and translation, often leading to reduced growth rate in plasmid-bearing strains and significant alterations in normal metabolism (Jones et al., 2000; Flores et al., 2004; Rozkov et al., 2004). For example, IPTG induced expression of *S. cerevisiae* α -glucosidase gene (*glucC*) inhibited the glucose uptake and respiration capacities in *E. coli* (Neubauer et al., 2003). Presence of plasmid containing a hepatitis B antigen under the control of a CMV promoter in *E. coli* reduced the growth rate and biomass yield respectively by 24% and 7% with an increase in the overflow metabolism (Rozkov et al., 2004). High copy-number (more than 200) ColE1 plasmids in *E. coli* BL21 significantly reduced the growth and the glucose consumption rates along with additional alterations in the enzyme activities of central metabolic pathways (Wang et al., 2006). Moreover, antibiotics (used as selection markers) like tetracycline at a high but sub-inhibitory concentration led to global induction of proteins related to bacterial survival in *P. putida* KT2440 (Yun et al., 2006). These additional negative factors become very significant especially under nutrient limited and stress conditions.

To overcome these complications, one of the conventionally used approaches in *genetic engineering* is incorporating the genes into the genome of the target organism. This chapter describes characterization of genomic integration of *Synechococcus elongatus* PCC 6301 phosphoenolpyruvate carboxylase (*ppc*) gene and glucose catabolic pathways in P-solubilizing *Pseudomonas* P4.

8.1.1: P-solubilization properties of *Pseudomonas* P4

pA172A, a pBR322 derived vector, contained *ppc* gene of *S. elongatus* PCC 6301 under *tet* promoter of tetracycline resistance gene of pBR322 (Kodaki et al., 1985).



pA172A plasmid was used as a suicide vector to directly transform *Pseudomonas*. The transformant *Pseudomonas* P4 was selected based on efficient P-solubilization phenotype (Srivastava, 2002; Ph. D thesis). The genomic integration of pA172A in *Pseudomonas* P4 was confirmed by obtaining a 909bp PCR amplicon using the forward primer corresponding to pBR322 DNA and reverse primer corresponding to N-terminal part of the *ppc* gene.

Pseudomonas P4 solubilized RP by secreting high amounts of gluconic acid. In enterobacters, gluconic acid production appears to be merely a RP solubilizing mechanism and is induced by phosphate starvation in *E. asburiae* PSI3 and *E. herbicola* (Goldstein and Liu., 1987; Gyaneshwar et al., 1999). On the contrary, periplasmic glucose dehydrogenase (GDH) mediated gluconic acid formation contributes as a predominant constitutive glucose catabolic pathway in pseudomonads (Lessie and Phibbs, 1984). Hence, its metabolic role in *Pseudomonas* P4 was expected to be significantly different than other non-P-solubilizing pseudomonads. Understanding the genetic basis of P-solubilization has been proposed to be important in developing efficient PSMs (Gyaneshwar, 2002). Considering the distinct carbon metabolism in pseudomonads, it is necessary to characterize the biochemical basis of MPS ability.

8.2: EXPERIMENTAL DESIGN

The following experimental strategy was designed to trace the site of integration of pA172A in *Pseudomonas* P4 genome and analyze the biochemical basis of MPS phenotype.

8.2.1: Bacterial strains used in this study

Pseudomonad strains	Characteristics	Reference
<i>P. fluorescens</i> 13525	Wild Type	MTCC, Chandigarh
<i>Pseudomonas</i> P4	Native P-solubilizing isolate of fluorescent pseudomonads	This study

Table 8.1: List of bacterial strains used. The growth and maintenance conditions for both the pseudomonads were as given in Section 2.2. *Pseudomonas* P4 showed different pigmentation (bluish-green) on Pseudomonas agar plates unlike *P. fluorescens* 13525 (fluorescent green).

8.2.2: Genetic characterization

8.2.2.1: 16S rDNA characterization of *Pseudomonas* P4

Pseudomonas P4 genomic DNA was used as template for PCR amplification of ~1,100bp region of 16S rDNA gene using the standard universal primers 27F and 1107R, corresponding to 16S rDNA of *E. coli*, the sequences of which are as follows:

Primer	Nucleotide sequence
Forward Primer: 27F	5' GAG AGT TTG ATC CTG GCT CAG 3'
Reverse Primer: 1107R	5' GCT CGT TGC GGG ACT TAA CC 3'

The thermal profile set in the thermal cycler included annealing at 58°C for 30seconds, extension at 72°C for 90seconds with rest of the profile same as described in Section 2.4.9 (Table 2.6). The PCR product was then partially sequenced using 1107R primer (Section 2.4.10). The partial 16S rDNA sequence was deposited to the GenBank and was subjected to standard bioinformatics tool for closest homology search.

8.2.2.2: Tracing the site of integration of pA172A into *Pseudomonas* P4 genome

Two possible mechanisms for the integration of *ppc* containing pA172A plasmid in *Pseudomonas* genome were site specific homologous recombination or random illegitimate recombination. Schematic representation of pA172A plasmid recovery from *Pseudomonas* P4 generated by either of the above mentioned recombination events is depicted in Fig. 8.1.

8.2.2.2(i) Retrieval of the integrated pA172A plasmid from *Pseudomonas* P4 genome

Assuming the genomic integration to be a single recombination event, a strategy was designed to recover the integrated pA172A plasmid from *Pseudomonas* P4 to obtain small fragments of host genomic DNA (Fig. 8.1a and b), the sequence of which could indicate the site of integration of pA172A. Accordingly, *Pseudomonas* P4 genomic DNA was isolated (Section 2.4.1.3) and was subjected to complete restriction digestion using XbaI or ApaI enzyme, whose recognition site was absent in pA172A plasmid. The genomic digest was purified and subjected to purification and self ligation (Section 2.4.6 and 2.4.7). The ligation mixture was transformed in *E. coli* JM101 and the transformants were selected on LA plates containing ampicillin. The restriction digestion patterns of the plasmids recovered from these experiments were compared to that of pA172A.

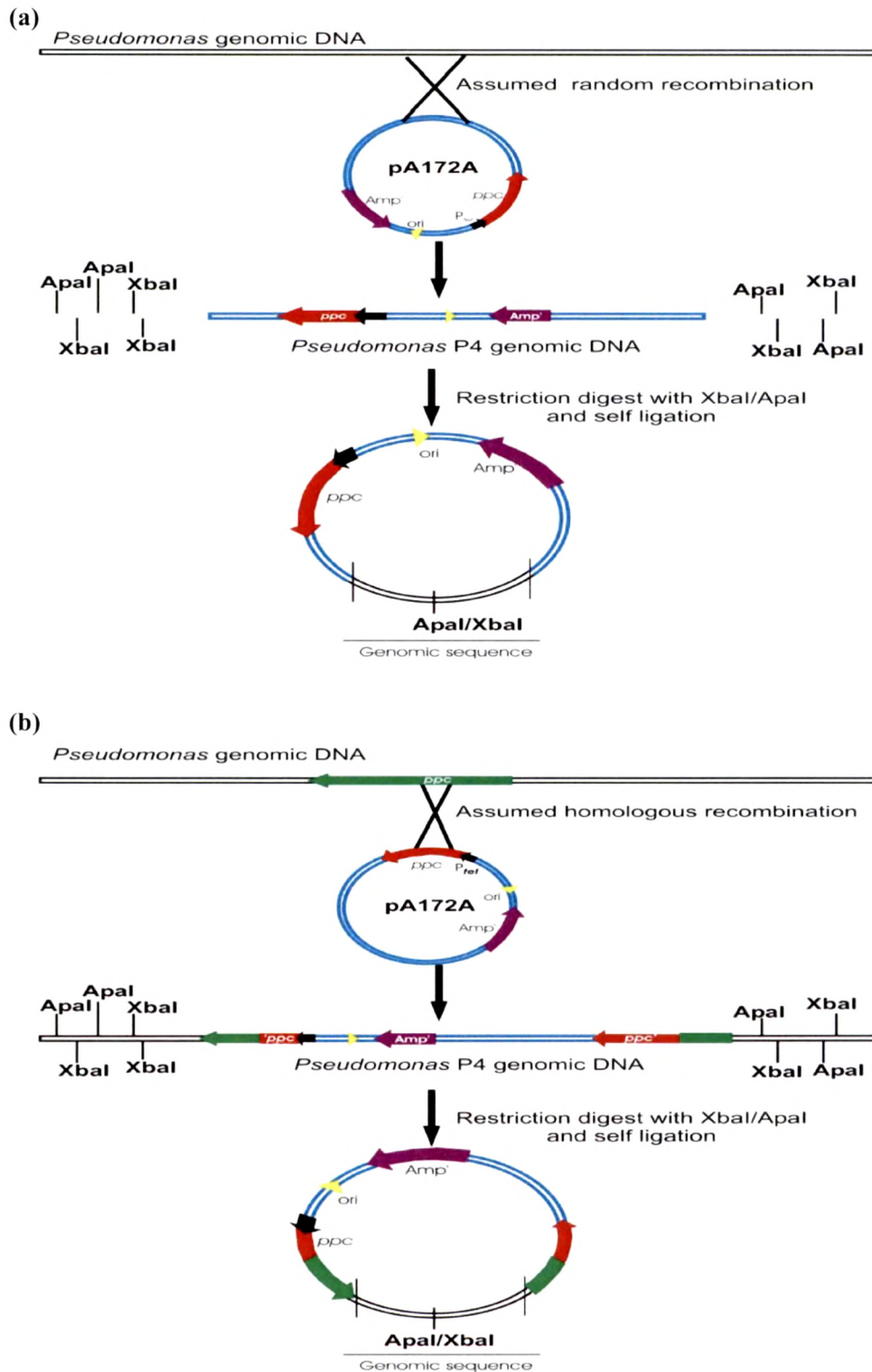
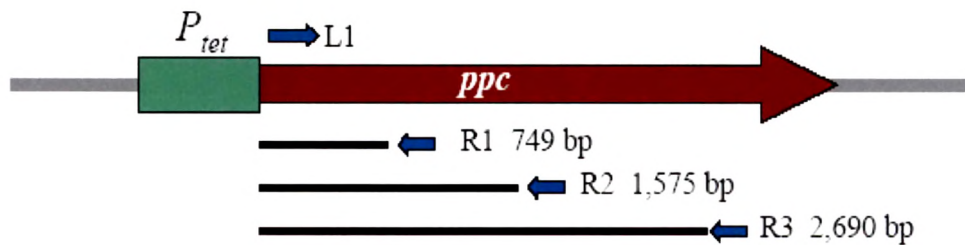


Fig. 8.1: Schematic representation of genomic integration event and expected map of the plasmids recovered from *Pseudomonas* P4 genome. (a) Random illegitimate recombination (b) Homologous recombination of *ppc* gene.

8.2.2.2(ii) Characterization of plasmids recovered from *Pseudomonas* P4 genome.

Confirmation of presence of *ppc* gene in the plasmids derived from genome

Randomly selected clones were checked for the presence of *ppc* gene by PCR amplification using the primers L1 and R1 corresponding to N-terminal region of the gene that produced 749bp amplicon. These positive clones were subjected to two further PCR amplifications to trace the presence of full-length *ppc* gene. For this, the forward primer L1 and the reverse primers R2 and R3 corresponding to intermediate and C-terminal regions of the *ppc* gene were used to produce 1,575bp and 2,690bp amplicons, respectively. Schematic representation of the PCR based strategy for characterizing the *ppc* gene along with the primer details and the specific requirements of the thermal profile are as shown in **Fig. 8.2**.



Set of primers used	Annealing temperature*	Extension time*	Expected amplicon size
L1R1	62°C, 56°C, 50 °C	60 seconds	749bp
L1R2	56°C	90 seconds	1,575bp
L1R3	50°C	150 seconds	2,690bp

Forward primer L1: 5' ATG AAT TAC TGC CAG AAC GCT CGA 3' (24 mer; % GC content=46%)

Reverse primer R1:- 5' CTG ACG AAT ATT CTG CGC TTC AAG 3' (24 mer; % GC content=46%)

Reverse primer R2:- 5' GCT TCG CTC AGC TCG TTG TA 3' (20 mer; % GC content=55%)

Reverse primer R3:- 5' GCA AAT CGA CCT TCG CTA GG 3' (20 mer; % GC content=55%)

Fig. 8.2: Characterization of *S. elongatus* PCC 6301 *ppc* gene in plasmids recovered from *Pseudomonas* P4 genome. PCR amplification was performed using common forward primer L1 in combination with three different reverse primers R1, R2 and R3 with the varying amplicon sizes are depicted as above. * Rest of the thermal profile for PCR program was same as described in Section 2.4.9. 15µl of the 50µl PCR system was subjected to agarose gel electrophoresis (Section 2.4.4).

Functional analysis of *ppc* gene in the plasmids derived from genome

Plasmids recovered from *Pseudomonas* P4 were transformed into *E. coli* JWK3928 (*ppc*⁻ strain) and the transformants were selected on kanamycin and ampicillin (Section 2.4.2.1; Table 2.4). The transformants were allowed to grow on M9 minimal medium containing glucose as carbon source in presence and absence of glutamate in order to check their ability to complement *ppc* mutation (Section 2.8).

Restriction mapping of the randomly selected plasmid derived from *Pseudomonas* P4 genome and determination of the sequence of genomic DNA fragment.

pA55 plasmid was randomly selected, from a set of plasmids showing the presence of 1,575bp *ppc* gene amplicon, for analyzing the restriction digestion patterns using 5 restriction enzymes like HindIII, BamHI, EcoRI, PstI and KpnI. The ~1.1kb BamHI unique fragment obtained from pA55 plasmid was ligated to the purified pBluescriptII SK(-) plasmid digested with BamHI to form pBSK(1.1) plasmid and the transformants were screened by blue-white selection (Section 2.4.2.1). The pBSK(1.1) plasmid isolated from a white colony was confirmed by restriction digestion and was subjected to DNA sequencing using standard M13 forward and reverse primers (Table 8.2) which gave 650bp and 335bp sequence information respectively (Section 2.4.1.1; 2.4.4; 2.4.5; 2.4.6; 2.4.10). The 650bp stretch was used to design yet another forward primer (I-1) to sequence remaining intermediate region. Arranging the overlapping regions of the three sequence stretches, finally 1,244bp DNA sequence was obtained. On the other hand, the ~5.4kb backbone of pA55 was subjected to self-ligation and the transformants were selected for ampicillin resistance (Fig. 8.3).

Primer	Nucleotide sequence	Comments
M13-u	5'-GTT TTC CCA GTC ACG AC-3'	M13 universal primer for pBluescriptII vectors, used for sequencing
M13-r	5'-AAC AGC TAT GAC CAT G-3'	M13 reverse primer for pBluescriptII vectors, used for sequencing
I-1	5'-TAT GCT GCC AGA AGA TGT CG-3' (20 -mer, %GC content=50%, T _m =60°C)	Designed for sequencing the intermediate region of ~1.1kb genomic DNA

Table 8.2: Oligonucleotides used for sequencing the ~1.1kb *Pseudomonas* P4 genomic DNA. The M13 primers are standard as described above in the text. Oligo-synthesis of the I-1 primer and the sequencing services were availed from MWG Biotech Pvt. Ltd.

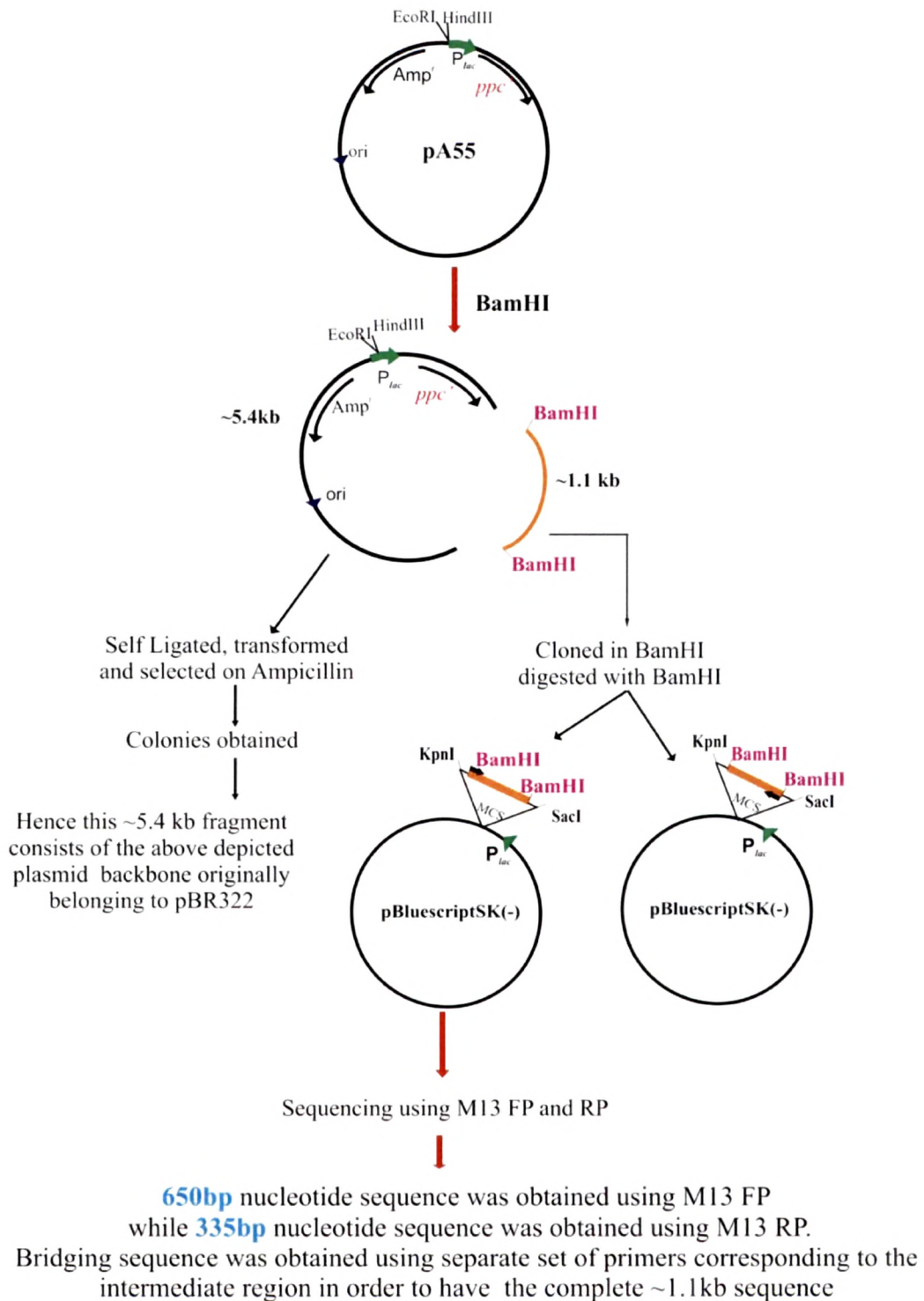


Fig. 8.3: Schematic representation of the methodology followed for identifying the sequence of *Pseudomonas* P4 genomic DNA fragment.

8.2.3: Phenotypic characterization

8.2.3.1: P-solubilizing ability of *Pseudomonas* P4 as compared to *P. fluorescens* 13525

The P-solubilization ability of *Pseudomonas* P4 was checked along with a standard non-P-solubilizing strain *P. fluorescens* 13525 on Pikovaskya's agar as well as on TRP agar (Tris buffered RP) plates (Section 2.2.4; 2.2.5; 2.7). The organic acid(s) secreted by these strains on TRP liquid medium were analyzed and quantified by HPLC (Section 2.2.4; 2.7; 2.9.3).

8.2.3.2: Effect of *Pseudomonas* P4 inoculation on growth and development of mung bean (*Vigna radiata*)

On account of efficient organic acid secretion and P-solubilization, *Pseudomonas* P4 was tested for its plant growth promoting ability using mung bean. Germinated mung bean seeds coated with *Pseudomonas* P4 culture were planted in 50ml MS agar constituted to provide P-sufficient and -limiting conditions with glucose and sucrose supplemented as carbon sources (Section 2.2.6; 2.12). The plant growth was monitored for 5-7 days in order to monitor the effect of *Pseudomonas* P4 inoculation.

8.2.4: Biochemical characterization

8.2.4.1: Growth and organic acid secretion in presence of varying Pi concentrations

Pseudomonas P4 and *P. fluorescens* 13525 were subjected to batch cultivation on Tris (pH=8.0) buffered minimal medium containing 100mM glucose as the sole carbon source and KH_2PO_4 as the source of Pi (Section 2.2.4). The growth and media acidification profiles as indicated by media pH values, were obtained on Pi levels corresponding to 1mg/ml RP (insoluble P source) and 0.1mM, 1.0mM, 10mM and 20mM of KH_2PO_4 (Section 2.9). Similar studies were carried out using both the *Pseudomonas* strains on M9 minimal medium (Section 2.9).

8.2.4.2: Physiology and glucose metabolism under P-deficient and -sufficient conditions

The growth, glucose utilization and organic acid production of *Pseudomonas* P4 and *P. fluorescens* 13525 were studied using TRP and M9 minimal media as P-deficient

and -sufficient conditions, respectively (Section 2.2.3; 2.2.4; 2.9). The processing of the experimental samples and calculations of the physiological parameters like specific growth rate, total glucose utilization rate, glucose uptake and organic acid yields was carried out as described in Section 2.9.3. The PPC, PYC, G-6-PDH and GDH activities under both the conditions were determined as described in Section 2.10.

8.3: RESULTS

Genetic characterization

8.3.1: 16S rRNA gene sequence of *Pseudomonas* P4

Primary fluorescence based selection of the isolate on *Pseudomonas* agar suggested that the organism belonged to the broad class of fluorescent pseudomonads. For further characterization, 16S rDNA was amplified (Section 8.2.2.1) and the 755bp partial sequence was obtained which is given in **Fig. 8.4a**.

Analysis of this sequence using NCBI-BLAST (Basic Local Alignment Search Tool) and Ribosomal Database Project (RDP) II, online homology search programs, revealed maximum identity (99%) to *Pseudomonas aeruginosa* sp. (Section 2.4.11; **Fig. 8.4b and c**). The GenBank accession number obtained for this partial 16S rDNA sequence is [EU224277](https://www.ncbi.nlm.nih.gov/nucl/224277) and the accession profile is given in **Fig. 8.5**.

```
ACGACAGCCATGCAGCACCTGTGTCTGAGCTCCCGAAGGCACAATCCATCTCTGGAAAGTTCTCAG
CATGTCAAGGCCAGGTAAGGTTCTTCGCGTTGCTTCGAATTAAACCACATGCTCCACCGCTTGTGC
GGGCCCCCGTCAATTCATTTGAGTTTTAACCTTGCGCCGTAAGTCCCGAGGCGGTGACTTATCGCG
TTAGCTGCGCCACTAAGATCTCAAGGATCCCAACGGCTAGTCGACATCGTTTACGGCGTGGACTAC
CAGGGTATCTAATCCTGTTTGTCTCCACGCTTTCGCACTCAGTGTGAGTATCAGTCCAGGTGGTC
GCCTTCGCCACTGGTGTTCCTTCCTATATCTACGCATTTACCGCTACACAGGAAATTCACCACCC
TCTACCGTACTCTAGCTCAGTAGTTTTGGATGCAGTTCACAGGTTGAGCCCGGGGATTTACATCCA
ACTTGCTGAACCACCTACGCGCGCTTACGCCCAGTAATCCGATTAACGCTTGCACCCTTCGTATT
ACCGCGGCTGCTGGCACGAAGTTAGCCGGTGCTTATTCTGTTGGTAACGTCAAACAGCAAGGTAT
TAACTTACTGCCCTTCCTCCCACTTAAAGTGCTTTACAATCCGAAGACCTTCTTCACACACGCGGC
ATGGCTGGATCAGGCTTTCGCCCATTTGCCAATATCCCACTGCTGCCTCCCGTAGGAGTCTGGAC
CGTGTCTCAGTTCAGTGTGAC
```

Fig. 8.4a: Partial 16S rDNA sequence of *Pseudomonas* P4

Sequences producing significant alignments:

Accession	Description	Total score	E value
EU302863.1	<i>Pseudomonas aeruginosa</i> strain DAP38 16S ribosomal RNA gene, partial sequence	1389	0.0
EU391426.1	<i>Pseudomonas aeruginosa</i> strain PBCC1 16S ribosomal RNA gene, partial sequence	1384	0.0
EU364810.1	<i>Pseudomonas aeruginosa</i> strain MG-P13 16S ribosomal RNA gene, partial sequence	1384	0.0
EU344794.1	<i>Pseudomonas aeruginosa</i> strain MML2212 16S ribosomal RNA gene, partial sequence	1384	0.0
EU352760.1	<i>Pseudomonas aeruginosa</i> strain NK 2 1B-1 16S ribosomal RNA gene, partial sequence	1384	0.0
DQ989211.2	<i>Pseudomonas aeruginosa</i> isolate IL1 16S ribosomal RNA gene, partial sequence	1384	0.0
EU331416.1	<i>Pseudomonas aeruginosa</i> strain pY11T-3-1 16S ribosomal RNA gene, partial sequence	1384	0.0
EU307934.1	<i>Pseudomonas</i> sp. 2-1 16S ribosomal RNA gene, partial sequence	1384	0.0
EU301769.1	<i>Pseudomonas outidis</i> strain G3 16S ribosomal RNA gene, partial sequence	1384	0.0
EU263017.1	<i>Pseudomonas aeruginosa</i> strain P2 16S ribosomal RNA gene, partial sequence	1384	0.0
EU259891.1	<i>Pseudomonas aeruginosa</i> strain SSC2 16S ribosomal RNA gene, partial sequence	1384	0.0
EU21384.1	<i>Pseudomonas aeruginosa</i> strain Y2P8 16S ribosomal RNA gene, partial sequence	1384	0.0
EU21383.1	<i>Pseudomonas aeruginosa</i> strain Y2P7 16S ribosomal RNA gene, partial sequence	1384	0.0
EU21382.1	<i>Pseudomonas aeruginosa</i> strain Y2P5 16S ribosomal RNA gene, partial sequence	1384	0.0
EU21381.1	<i>Pseudomonas aeruginosa</i> strain Y2P3 16S ribosomal RNA gene, partial sequence	1384	0.0
EU21380.1	<i>Pseudomonas aeruginosa</i> strain Y2P2 16S ribosomal RNA gene, partial sequence	1384	0.0
EU037286.1	<i>Pseudomonas</i> sp. G3DM-81 16S ribosomal RNA gene, partial sequence	1384	0.0
EU287481.1	<i>Pseudomonas</i> sp. J15 16S ribosomal RNA gene, partial sequence	1384	0.0
EF362637.1	<i>Pseudomonas aeruginosa</i> strain 8 16S ribosomal RNA gene, partial sequence	1384	0.0

```
> gb|EU302863.1 Pseudomonas aeruginosa strain DAP38 16S ribosomal RNA gene,
partial sequence
Length=1444

Score= 1389 bits (752), Expect= 0.0, Identities= 755/756 (99%), Gaps= 1/756 (0%)
Strand=Plus/Minus

Query 1      ACGACAGCCATGCAGCACCTGTGTCTGAGCTCCCGAAGGSCA-CAATCCATCTCTGGAAAG 59
Sbjct 999     ACGACAGCCATGCAGCACCTGTGTCTGAGCTCCCGAAGGSCACCAATCCATCTCTGGAAAG 940

Query 60     TTCTCAGCATGTCAAGGCCAGGTAAGGTTCTTCGCGTTGCTTCGAATTAARACCATGCT 119
Sbjct 939     TTCTCAGCATGTCAAGGCCAGGTAAGGTTCTTCGCGTTGCTTCGAATTAARACCATGCT 880

Query 120    CCACCGCTTGTGCGGGCCCCCGTCAATTCATTGAGTTTTAACCTTGCGGCCGTA CTCCC 179
Sbjct 879     CCACCGCTTGTGCGGGCCCCCGTCAATTCATTGAGTTTTAACCTTGCGGCCGTA CTCCC 820

Query 180    CAGGCGGTTCGACTTATCGCGTTAGCTGCGCCACTAAGATCTCAAGGATCCCAACGGCTAG 239
Sbjct 819     CAGGCGGTTCGACTTATCGCGTTAGCTGCGCCACTAAGATCTCAAGGATCCCAACGGCTAG 760

Query 240    TCGACATCGTTTACGGCGTGGACTACCAAGGGTATCTAATCCTGTTTGCTCCCCACGCTTT 299
Sbjct 759     TCGACATCGTTTACGGCGTGGACTACCAAGGGTATCTAATCCTGTTTGCTCCCCACGCTTT 700

Query 300    CGCACCTCAGTGTCAATCAGTCCAGGTGGTGCCTTCGCCACTGGTGTTCCTTCCTAT 359
Sbjct 699     CGCACCTCAGTGTCAATCAGTCCAGGTGGTGCCTTCGCCACTGGTGTTCCTTCCTAT 640

Query 360    ATCTACGCATTTACCGCTACACAGGAAATCCACCACCTCTACCGTACTCTAGCTCAG 419
Sbjct 639     ATCTACGCATTTACCGCTACACAGGAAATCCACCACCTCTACCGTACTCTAGCTCAG 580

Query 420    TAGTTTTGGATGCAGTTCCAGGTTGAGCCCGGGGATTTACATCCAACTTGCTGAACCA 479
Sbjct 579     TAGTTTTGGATGCAGTTCCAGGTTGAGCCCGGGGATTTACATCCAACTTGCTGAACCA 520

Query 480    CCTACGCGCGCTTTACGCCAGTAATTCGGATTAAACGCTTGCAACCTTCGTAATTACCGCG 539
Sbjct 519     CCTACGCGCGCTTTACGCCAGTAATTCGGATTAAACGCTTGCAACCTTCGTAATTACCGCG 460

Query 540    GCTGCTGGCACGAAGTTAGCCGGTGCCTTATTCGTTGGTAACGTCAAAACAGCAAGGTAT 599
Sbjct 459     GCTGCTGGCACGAAGTTAGCCGGTGCCTTATTCGTTGGTAACGTCAAAACAGCAAGGTAT 400

Query 600    TAACITACTGCCCTTCTCCCAACTTAAAGTGCTTTACAATCCGAAGACCTTCTTCACAC 659
Sbjct 399     TAACITACTGCCCTTCTCCCAACTTAAAGTGCTTTACAATCCGAAGACCTTCTTCACAC 340

Query 660    ACGCGGCATGGCTGGATCAGGCTTTCGCCCATTTGTCCAATATTCCTCCACTGCTGCCTCCC 719
Sbjct 339     ACGCGGCATGGCTGGATCAGGCTTTCGCCCATTTGTCCAATATTCCTCCACTGCTGCCTCCC 280

Query 720    GTAGGAGTCTGGACCGTGTCTCAGTTCAGTGTGAC 755
Sbjct 279     GTAGGAGTCTGGACCGTGTCTCAGTTCAGTGTGAC 244
```

Fig. 8.4(b): Homology search result of partial 16S rDNA of *Pseudomonas* P4 using NCBI-BLAST

Match hit format: short ID, orientation, similarity score, S_ab score, unique common oligomers and sequence full name.

Lineage:

Results for Query Sequence: unknown, 733 unique oligos

domain Bacteria (20) (match sequences)

- phylum Proteobacteria (20)
 - class Gammaproteobacteria (20)
 - order Pseudomonadales (20)
 - family Pseudomonadaceae (20)
 - genus *Pseudomonas* (20)

S000002377	not_calculated	0.988	1459	<i>Pseudomonas aeruginosa</i> ; AL98; AJ249451
S000005690	not_calculated	0.988	1406	<i>Pseudomonas aeruginosa</i> ; 42A2 NCBI 40045; AJ309500
S000008931	not_calculated	0.988	1452	<i>Pseudomonas</i> sp.; DLB-1; AJ387904
S000255100	not_calculated	0.988	1456	<i>Pseudomonas aeruginosa</i> ; AB126582
S000333003	not_calculated	0.988	1421	<i>Pseudomonas aeruginosa</i> ; X13; AY631241
S000358771	not_calculated	0.988	1393	<i>Pseudomonas aeruginosa</i> ; AU0416; AY486350
S000358775	not_calculated	0.988	1382	<i>Pseudomonas aeruginosa</i> ; AU1883; AY486354
S000384534	not_calculated	0.988	1460	<i>Pseudomonas aeruginosa</i> ; AB073312
S000386060	not_calculated	0.988	1458	<i>Pseudomonas aeruginosa</i> ; WatG; AB117953
S000388353	not_calculated	0.988	1391	<i>Pseudomonas aeruginosa</i> ; 86351; AF157689
S000388896	not_calculated	0.988	1449	<i>Pseudomonas aeruginosa</i> ; MF1; AF193514
S000389575	not_calculated	0.988	1434	bacterium str. 61716; AF227866
S000412778	not_calculated	0.988	1457	<i>Pseudomonas aeruginosa</i> ; Z5; AY548952
S000412779	not_calculated	0.988	1457	<i>Pseudomonas aeruginosa</i> ; Z11; AY548953
S000428754	not_calculated	0.988	1416	<i>Pseudomonas aeruginosa</i> ; ATCC 10145; AF094713
S000428757	not_calculated	0.988	1330	<i>Pseudomonas aeruginosa</i> ; ATCC 27316; AF094716
S000428759	not_calculated	0.988	1400	<i>Pseudomonas aeruginosa</i> ; ATCC 15442; AF094718
S000428761	not_calculated	0.988	1400	<i>Pseudomonas aeruginosa</i> ; ATCC 33350; AF094720
S000458490	not_calculated	0.988	1460	<i>Pseudomonas</i> sp. pDL01; AF125317
S000497702	not_calculated	0.988	1461	<i>Pseudomonas aeruginosa</i> PA01; AE004501

Fig. 8.4(c): Homology search result of partial 16S rDNA of *Pseudomonas P4* using RDP II

LOCUS	EU224277	755 bp	DNA	linear	BCT 06-NOV-2007
DEFINITION	<i>Pseudomonas aeruginosa</i> strain P4 16S ribosomal RNA gene, partial sequence.				
ACCESSION	EU224277				
VERSION	EU224277.1 GI:158969745				
KEYWORDS	.				
SOURCE	<i>Pseudomonas aeruginosa</i>				
ORGANISM	<i>Pseudomonas aeruginosa</i> Bacteria; Proteobacteria; Gammaproteobacteria; Pseudomonadales; Pseudomonadaceae; <i>Pseudomonas</i> .				
REFERENCE	1 (bases 1 to 755)				
AUTHORS	Buch, A.D., Naresh Kumar, G. and Archana, G.				
TITLE	Partial 16S rDNA sequence of <i>Pseudomonas P4</i>				
JOURNAL	Unpublished				
REFERENCE	2 (bases 1 to 755)				
AUTHORS	Buch, A.D., Naresh Kumar, G. and Archana, G.				
TITLE	Direct Submission				
JOURNAL	Submitted (17-OCT-2007) Department of Biochemistry, M. S. University of Baroda, Vadodara, Gujarat 390002, India				
FEATURES	Location/Qualifiers				
source	1..755 /organism="Pseudomonas aeruginosa" /mol_type="genomic DNA" /strain="P4" /db_xref="taxon:287" <1..>755 /product="16S ribosomal RNA"				
<u>rRNA</u>					
ORIGIN	1 gtcacactgg aactgagaca cggctccagac tctctacggga ggcagcagtg gggaaatattg 61 gacaatgggc gaaagcctga tccagccatg cgcgctgtgt gaagaaggtc ttcggattgt 121 aaagcacttt aagttgggag gaagggcagt aagttaatac cttgctgttt tgacgttacc 181 aacagaataa gcaccggcta acttcgtgccc agcagccgag gtaatacga ggggtgcaagc 241 gttaatcgga attactgggc gtaaagggcg cgtaggtggt tcagcaagtt ggatgtgaaa 301 tccccgggct caacctggga actgcatcca aaactactga gctagagtc ggttagagggg 361 ggtggaattt cctgtgttagc ggtgaaatgc gtagatatag gaaggaacac cagtggcgaa 421 ggcgaccacc tggactgata ctgacactga ggtgcaaaag cgtggggagc aaacaggatt 481 agataccctg gtagtccacg ccgtaaacga tgttcgactag ccgttgggat ccttgagatc 541 ttagtggcgc agctaaccgc ataatgtagc cgcctggggg gtacggccgc aaggttaaaa 601 ctcaaatgaa ttgacggggg cccgcacaag cgggtggagca tgtggtttaa ttcgaagcaa 661 cggaagaac cttacctggc cttgacatgc tgagaacttt ccagagatgg attgtgcctt 721 cgggagctca gacacaggtg ctgcatggct gtcgt				

Fig. 8.5: GenBank accession result of partial 16S rDNA sequence of *Pseudomonas P4*

8.3.2: Investigation of the *ppc* gene integration site in *Pseudomonas* P4 genome

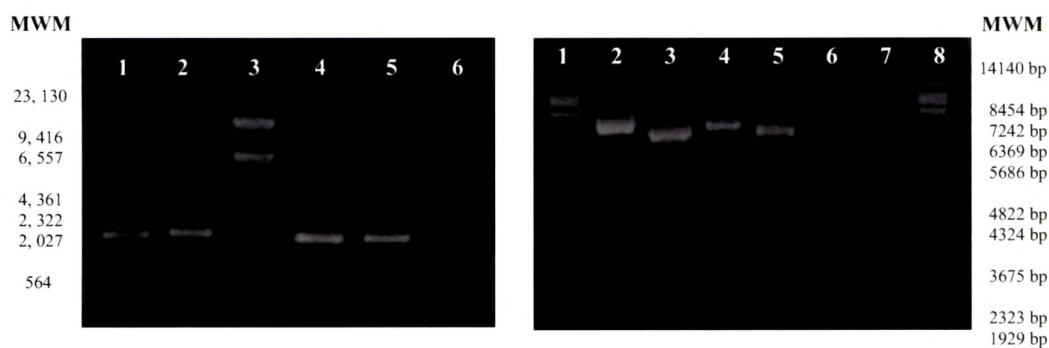
The strategies followed for tracing the site of integration of pA172A have been described in Section 8.2.2.2.

8.3.2.1: pA172A recovery from *Pseudomonas* P4 genomic DNA and characterization of the recovered plasmids

50-150 ampicillin resistant colonies were obtained from the transformation of the XbaI and ApaI digested genomic DNA of *Pseudomonas* P4. Similarly processed *P. fluorescens* 13525 genomic DNA was used as negative control, which did not form any ampicillin resistant colonies. Three randomly selected clones obtained from XbaI digested genomic DNA designated as pA21, pA22 and pA23 were characterized further. PCR of these three plasmids using the primers L1 and R1 of *ppc* gene showed the presence of ~800bp amplicon (Fig. 8.6a).

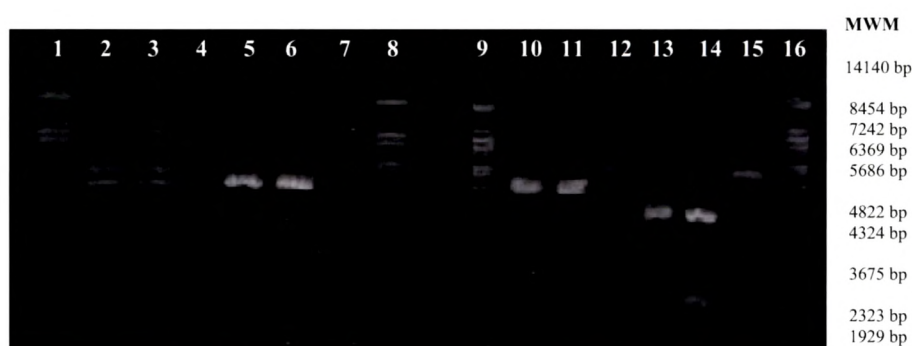
The restriction digestion profiles of pA21, pA22 and pA23 (Fig. 8.6b and c) indicated variation from the pA172A plasmid but the size of the genomic fragment was not very clear. Surprisingly the sizes of all the three plasmids were found to be approximately 5-6kb which was less than pA172A plasmid size of ~8.0kb. Amongst them, pA23 showed the maximum plasmid size and hence was subjected to DNA sequencing using a 20 -mer primer (5' AAG CGC AGA ATA TTC GTC AG 3'; Microsynth AG, Switzerland) suitable to sequence the region ahead of the initial ~800bp region of *ppc* gene which was already detected by PCR amplification. The sequencing reaction although failed to give clear details of the targeted DNA sequence in the plasmid but could only confirm the presence of *E. coli* origin of replication and β -lactamase gene in pA23. These details further confirmed the integration of pA172A in *Pseudomonas* genome.

Another set of 10 clones, recovered from ApaI and XbaI digested *Pseudomonas* P4 genomic DNA, was selected on the basis of presence of PCR amplicon using L1R1 set of primers and were analyzed further. These clones were designated as pA2, pA18, pA51, pA55, pA56, pX2, pX6, pX15, pX20 and pX25. The restriction digestion patterns of these plasmids compared with pA172A revealed that the sizes of these plasmids ranged between 4-7kb and were less than the 8.0kb size of pA172A plasmid (Fig. 8.7).



(a) Lane 1: pA21 amplified using L1R1; Lane 2: pA22 amplified using L1R1; Lane 3: Molecular weight marker-λ DNA digested with HindIII; Lane 4: pA23 amplified using L1R1; Lane 5: pA172A amplified using L1R1; Lane 6: pBR322 amplified using L1R1

(b) Lane 1 and 8: Molecular weight marker (MWM) – λ DNA digested with BstEII; Lane 2: pA21 digested with KpnI; Lane 3: pA21 digested with EcoRI/BamHI; Lane 4: pA22 digested with KpnI; Lane 5: pA22 digested with EcoRI/BamHI; Lane 6: pA23 digested with KpnI; Lane 7: pA23 digested with EcoRI/BamHI



(c) Lanes 1, 8, 9 and 16: MWM- λDNA digested with BstEII; Lane 2: pA21 digested with HindIII; Lane 3: pA22 digested with HindIII; Lane 4: pA23 digested with HindIII; Lane 5: pA21 digested with Sall; Lane 6: pA22 digested with Sall; Lane 7: pA23 digested with Sall; Lane 10: pA21 digested with XbaI/XhoI; Lane 11: pA22 digested with XbaI/XhoI; Lane 12: pA23 digested with XbaI/XhoI; Lane 13: pA21 digested with ScaI/EcoRI; Lane 14: pA22 digested with ScaI/EcoRI; Lane 15: pA23 digested with ScaI/EcoRI

Fig. 8.6: PCR amplification and restriction mapping of pA21, pA22 and pA23. (a) depicts the PCR amplification profile using L1 and R1 primers for *ppc* gene while (b) and (c) describe the restriction digestion patterns of three plasmids

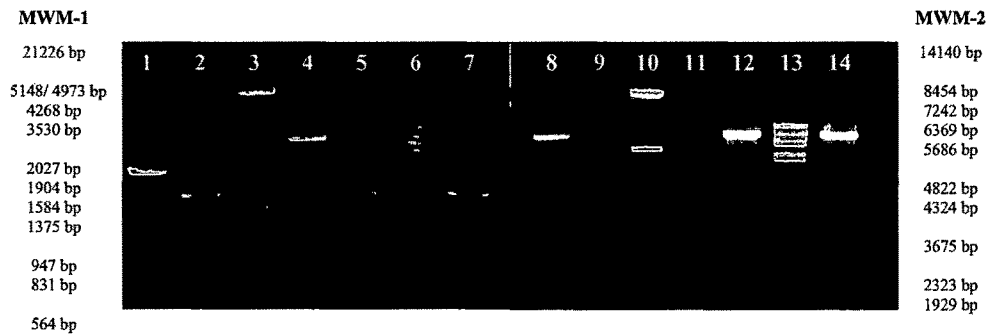


Fig. 8.7: Size determination of selected 10 clones derived from XbaI and ApaI digested *Pseudomonas P4* genomic DNA. Lanes 1, 2, 4, 5 and 7: pA2, pA18, pA55, pA51 and pA56 digested with ApaI; Lanes 8, 9, 11, 12 and 14: pX2, pX6, pX15, pX20 and pX25 digested with XbaI; Lanes 3 and 10: Molecular weight marker (MWM-1) - λ DNA digested with EcoRI and HindIII; Lanes 6 and 13: MWM-2- λ DNA digested with BstEII

8.3.2.2: Characterization of *ppc* gene insert in the 10 selected clones derived from *Pseudomonas P4* genome

The PCR based strategy (Section 8.2.2.2) used to “walk” along *ppc* gene demonstrated that apart from showing the presence of PCR amplicon using L1 and R1 primers, all 10 clones showed amplification with L1R2 set of primers but not with L1R3 set of primers (Table 8.3, Fig. 8.8). Identical results were obtained with *Pseudomonas P4* genomic DNA amplification using these primers. All these plasmids could not complement the glutamate auxotrophy of *E. coli* JWK3928 (*ppc* mutant) (Section 8.2.2.2(ii); Fig. 8.9). Collectively these results suggested the presence of *S. elongatus ppc* gene in truncated form in *Pseudomonas P4* which was consistently demonstrated in the plasmids derived from the genome.

<i>Pseudomonas P4</i> genome derived clones	Primer combinations			<i>Pseudomonas P4</i> genome derived clones	Primer combinations		
	L1R1	L1R2*	L1R3		L1R1	L1R2*	L1R3
pX2	+	+	-	pA2	+	+	-
pX6	+	+	-	pA18	+	+	-
pX15	+	+	-	pA51	+	+	-
pX20	+	+	-	pA55	+	+	-
pX25	+	+	-	pA56	+	+	-
pBR322	-	-	-	P4 genomic DNA	+	+	-
pA172A	+	+	+				

Table 8.3: Summarized results of PCR based examination of *ppc* gene in plasmids derived from *Pseudomonas P4* genome. PCR conditions and other details are specified in Fig. 8.2. *Amplicons using L1R2 set of primers were very faintly visible.

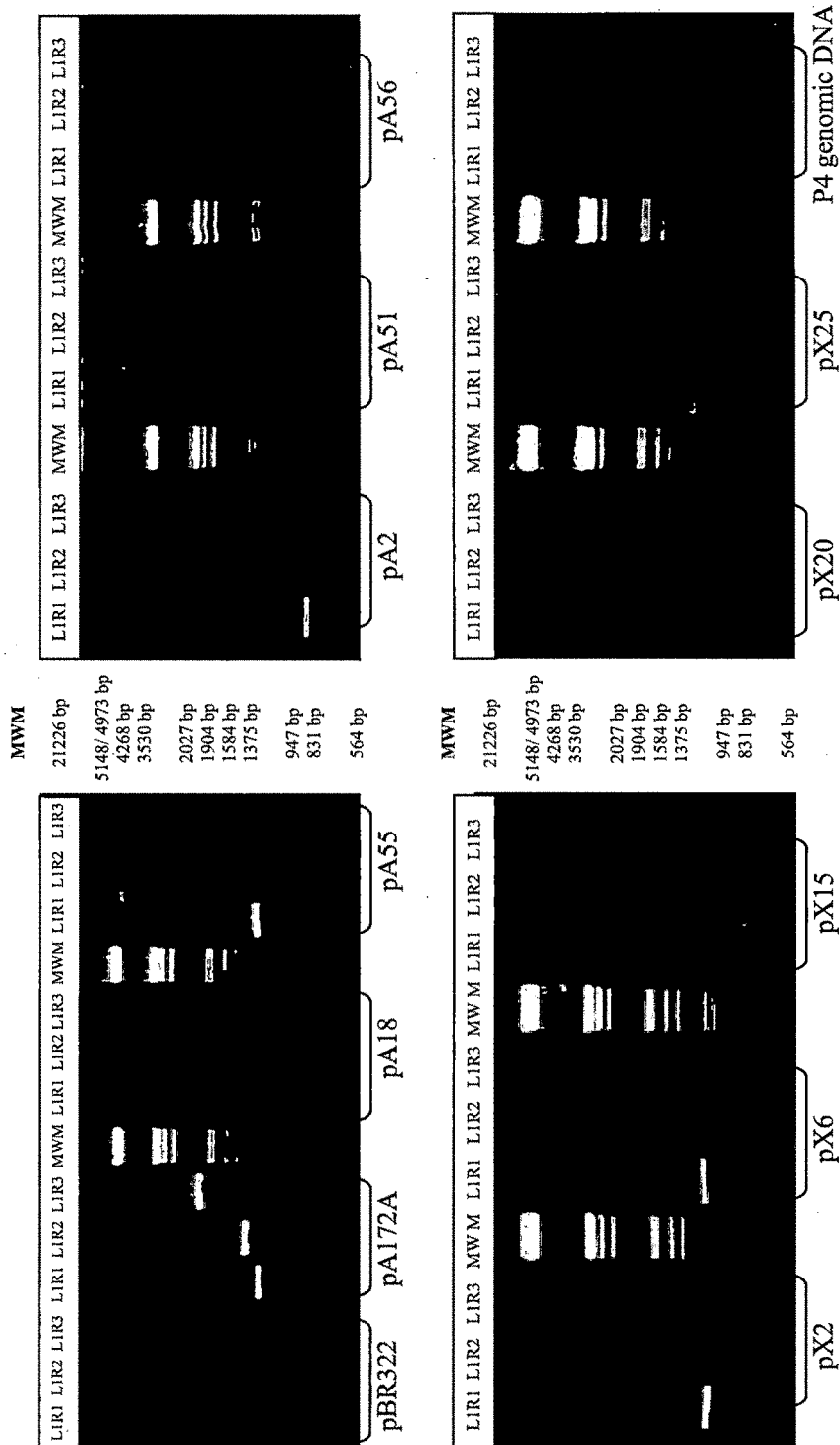


Fig. 8.8: PCR amplification of 10 plasmids derived from *Pseudomonas* P4 genome to examine the presence of full-length *ppc* gene. L1R1, L1R2 and L1R3 indicate the PCR amplicons obtained with respective sets of forward and reverse primers as discussed in text. The triplet of PCR amplicons for each clone is marked underneath. pA172A and pBR322 plasmids were used as positive and negative controls respectively. The λ DNAs double digested with EcoRI-HindIII was used as the DNA molecular weight marker (MWM). The experimental details are described in the Section 8.2.2.2(ii); Fig. 8.2.

Engineering the glucose metabolism of *Pseudomonas* spp. by heterologous expression of phosphoenolpyruvate carboxylase (PPC) and citrate synthase (CS) gene

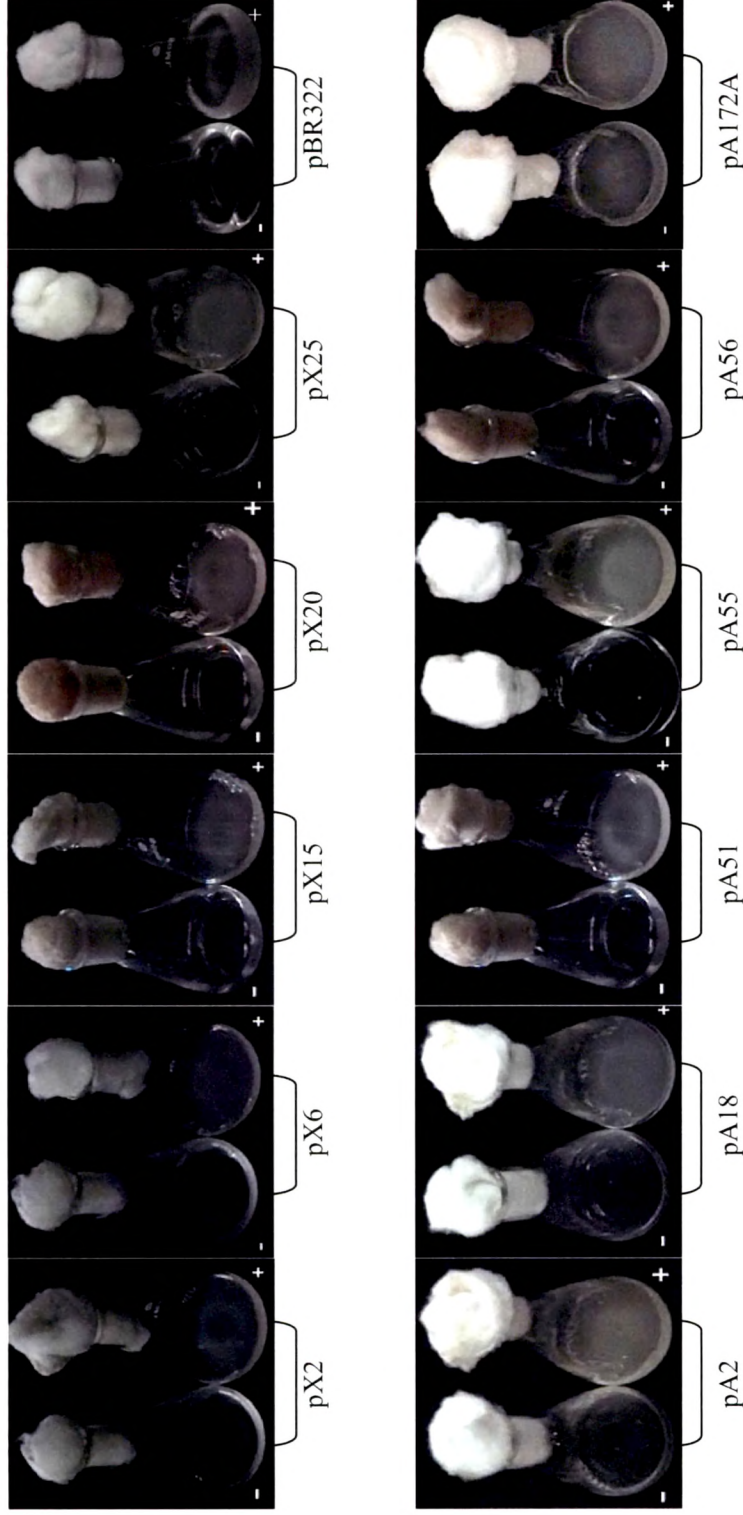


Fig. 8.9: *E. coli* JWK3928 complementation phenotype of the plasmids derived from *Pseudomonas P4* genome. *E. coli* JWK3928 transformants of individual plasmids were grown on M9 minimal medium containing glucose in presence and absence of 340µg/ml glutamate for 48-72 hours as described in Section 2.8. The - and + signs at the corners of each picture depict the growth of *E. coli* JWK3928 transformants in absence and presence of glutamate. Transformants of pBR322 and pA172A were used as negative and positive controls respectively.

8.3.3: Restriction mapping of randomly selected pA55

Due to maximum apparent plasmid size, pA55 plasmid was selected for restriction mapping. Restriction digestion profile of pA55 plasmid showed that EcoRI, KpnI, HindIII and XbaI enzymes linearized pA55 plasmid (**Fig. 8.10**) whereas BamHI generated two bands corresponding to ~1.1kb and ~5.4kb sizes. This band pattern observed was distinct from pA172A plasmid which produced a single band when digested with BamHI. This suggested that at least one BamHI site was contributed by the genomic DNA fragment retrieved from *Pseudomonas P4*.

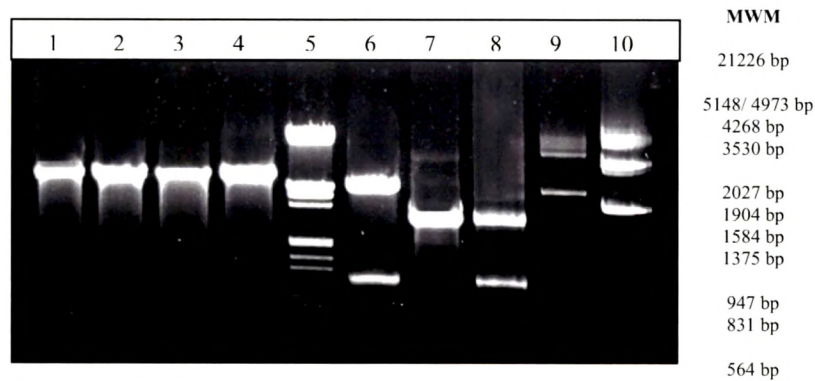


Fig. 8.10: Restriction mapping of pA55 plasmid. Lane1: pA55 digested with EcoRI; Lane2: pA55 digested with XbaI; Lane3- pA55 digested with HindIII; Lane4 - pA55 digested with KpnI; Lane 5- Molecular weight marker (MWM)- λ DNA double digested with EcoRI and BamHI; Lane6- pA55 digested with BamHI; Lane7- pBluescriptSK(-) digested with BamHI; Lane8- pBSK(1.1) digested with BamHI (~5.4kb and ~1.1kb); Lane9- undigested pA55 plasmid; Lane10- undigested pBSK(1.1) plasmid.

8.3.4: Determination of pA55 derived *Pseudomonas P4* genomic DNA sequence

The ~1.1kb genomic DNA fragment of *Pseudomonas P4* obtained from pA55, plasmid was incorporated in pBluescriptSK(-) at BamHI site and was used to derive the nucleotide sequence which would correspond to some sequence in *Pseudomonas P4* genome (described in detail in Section 8.2.2.2(ii)). On the other hand, development of ampicillin resistant colonies by transformation of self ligated ~5.4kb fragment of BamHI digested pA55 also confirmed that the ~5.4kb fragment belonged to the vector backbone while ~1.1kb DNA fragment was obtained from *Pseudomonas* genome. The nucleotide sequence of ~1.1kb fragment is given in **Fig. 8.11**.

```

CGGAATTGGGTACCGGGCCCCCCCCTCGAGGTCGACGGTATCGATAAGCTTGATATCGAATTCCTG
CAGCCCGGGGGATCCTTACAAACTGCACGCCGGTATGGCCTTCGTCAGTCTGAAACCGTGGGAAGAGC
GTAATGGTGACGAAAAACAGTGCGGAAGCGGTAATCCATCGTGCCAAAATGGAATTGGGCAAGATCCGC
GACGGTTTTGTCAATTCATTCAATATGCCAGCCATTGTTGAACTGGGCACGGCAACGGGTTTCGACTTTG
AGTTAATTGATCAGGCTGGGCTGGGTACGATGCCCTAACCCAGGCCCGTAACCAGTTGCTTGGTATGGC
GGCGCAACATCCTGCCAGCTTAGTCAGCGTGCCCTAATGGCCTGGAAGACACCGCGCAGTTAAACT
GGAAGTTGACCAGGAAAAGGCGCAGGCATTAGGTGTTTCACTTTCTGACATCAATCAGACCATTTCAAC
GGCGCTGGGTGGGACTTACGTTAACGACTTCATCGACCGTGGCCGCGTGAAAAAGTTGTATGTTTCAGGC
GGATGCCAAATTCGGTATGCTGCCAGAAGATGTCGATAAACTTTATGTCCGCAGCGCCAACGGCGAAAT
GGTGCCATTCTCGGCCTTTACCACTTCACATTGGGTGTATGGCTCTCCGCGACTGGAACGCTACAACGGT
CTGCCGTCAATGGAGATTGAGGGGGAAGCCGCGCCAGGGAACAGTTCCGGCGATGCCATGGCGTTGAT
GGAAAACCTTGCCTCGAAATTACCTGCGGGCATTGGTTATGACTGGACGGGTATGTCGTATCAGGAACG
CTTATCGGGAAACCAGGCTCCCCTCTGGTAGCAATTCCTTTGTGGTTGTTTTCTGTGCCTTGCTGCAC
TCTATGAAAGCTGGTCAATTCCTGTCTCGGTTATGTTGGTAGTGCCGTTAGGGATTGTCGGCGTGCTGCT
GGCGGCGACTCTTTAATCAAAAAAATGACGTCTACTTTATGGTGGGCTTGCTAACGACAATTGGCTTG
TCGGCCAAAACGCTATTTTGATCGTTGAGTTCGCTAAAAGATCTCATGGAGAAAAGAGGGTAAAGGTGTT
GTTGAAGCGACTGATGGCAGTACGTATGCGTCTGCGTCTATCCTGATGACCTCTCTCGCCTTATTCT
CGGCGTATTACCGCTAGCTATCAGTAACGGTGCCGGCAGTGGCGCGCAGAACGCTGTGGGTATCGGGGT
AATGGGGGAGGAATGGTCTCTGCAACGTTGCGGGCAATCTCTTTAATACCGCGCTGCAGTTGTAAAGG
ATCCACTAGTTCTAGAGCGGCCGCCACCGCGGTGGAGCTCCAGCTTTGTTCCCTTAGTGAGGGT
TAATTCGAG

```

Figure 8.11: DNA sequence of the ~1.1kb *Pseudomonas* P4 genomic DNA fragment. Grey highlighted nucleotides at the two ends correspond to the pBluescriptSK(-) backbone. The ~1.1kb DNA was sequenced from the both directions using standard M13 forward and reverse primers (Table 8.2), to obtain 650bp and 335bp nucleotide sequences, respectively. The intermediate sequence was obtained using another primer designed based on 650bp sequence to read in the forward direction. The overlaps in the resultant three patches of nucleotide sequences were arranged in order to have the complete 1, 244bp sequence of *Pseudomonas* P4 genome.

The online NCBI-BLAST homology search of the 1,244bp sequence using “megablast” revealed that it had high similarity with *E. coli* genomic DNA region corresponding to multi-drug efflux systems (Fig. 8.12). Homology search using “blastn” for nearly similar sequences selectively in *Pseudomonas* also revealed 66% identity with RND multidrug efflux transporter, MexB of *Pseudomonas aeruginosa* while 65% identity was found with hydrophobe/amphiphile efflux-1 system HAE1 in *P. fluorescens* PfO-1. No significant similarities were found with any of the known *ppc* or any glucose metabolism genes. Hence the mechanism of pA172A plasmid integration in *Pseudomonas* genome and the cause for the presence of truncated *ppc* gene are not clear.

Phenotypic characterization

8.3.5: P-solubilizing ability of *Pseudomonas* P4

Pseudomonas P4 showed very efficient di-calcium phosphate solubilization as observed on Pikovaskya's Agar (PVK) where it formed a prominent zone of clearance as compared to *P. fluorescens* 13525 (**Fig. 8.13**). Moreover, formation of intense red zone of acidification on buffered-RP agar plate also showed P solubilization ability of *Pseudomonas* P4.

Strong P-solubilizing ability of *Pseudomonas* P4 was also confirmed on buffered-RP broth where it acidified the media pH (=8.0) to less than 5 within 96-120h with a better growth status as compared to *P. fluorescens* 13525. *Pseudomonas* P4 secreted high levels of gluconic acid ($46\text{mM}\pm 3.96$) in the medium whereas *P. fluorescens* 13525 could only secrete very low amounts ($\sim 1\text{mM}$).

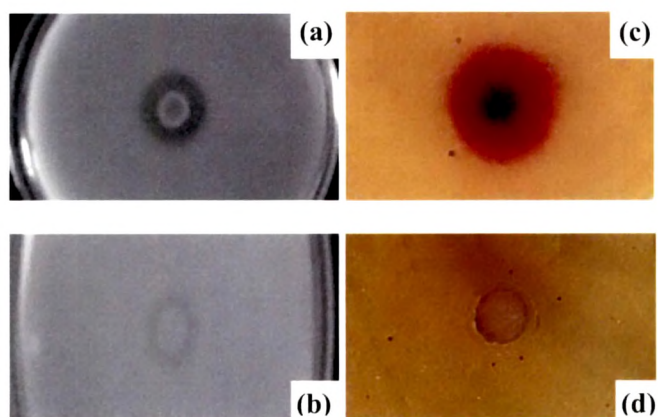


Fig. 8.13: P-solubilizing ability of *Pseudomonas* P4 and *P. fluorescens* 13525. (a), (b) depict formation of zone of clearance on PVK agar while (c), (d) show formation of zone of acidification on buffered TRP-methyl red agar by *Pseudomonas* P4 and *P. fluorescens* 13525. The media composition and experimental procedures were as described in text.

8.3.6: Plant inoculation studies using *Pseudomonas* P4

The effect of *Pseudomonas* P4 on the growth of mung bean (*Vigna radiata*) is summarized in **Table 8.4**. The un-inoculated MS and MS-RP controls showed healthy growth irrespective of presence or absence of AI (**Fig. 8.14**). However, in MS-P4-I and MS-RP-P4-I sets, *Pseudomonas* P4 overgrew and negatively affected the plant growth.

Growth condition		-Sucrose +100mM glucose		+1% sucrose, +100mM glucose	
		-Al	+400 μ M Al [#]	-Al	+400 μ M Al [#]
MS medium	Control	+++	+++	+++++	+++++
	P4-I	+++	+++	++*	++*
MS with RP	Control	++	-	+++++	+++++
	P4-I	+++	+++++	+++++	+++++

Table 8.4: Effect of *Pseudomonas* P4 on the growth of mung beans (*Vigna radiata*).

The experimental procedures are as described in the text. MS media composition and other experimental details are specified in Section 2.2.6 and 2.16. Control- uninoculated plants; P4-I- inoculated with *Pseudomonas* P4. [#] *Pseudomonas* P4 was demonstrated to be tolerant to 400 μ M Al (Ph. D thesis by Srivastava, S, 2002) *Plant growth after 4-5 days was negatively affected by overgrown *Pseudomonas* P4. Number of + indicates relative differences in plant growth.

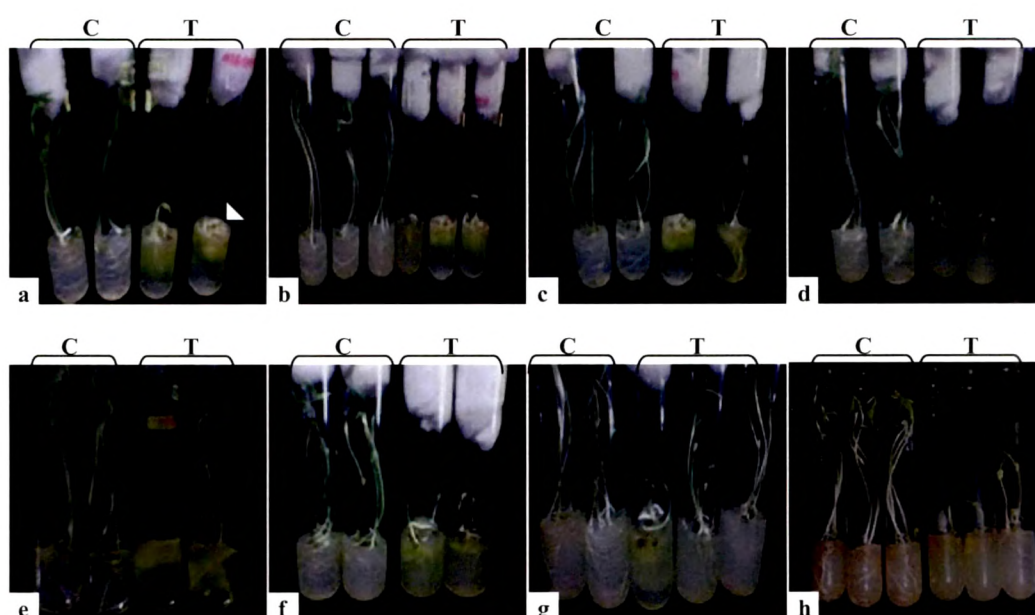


Fig. 8.14: Effect of *Pseudomonas* P4 inoculations on the growth of mung bean (*Vigna radiata*) under different experimental conditions. (a) Murashige-Skooge's (MS) medium + 100mM glucose (b) MS medium+100mM glucose+RP as sole P source (c) MS+100mM glucose+400 μ M AlCl₃ (d) MS+RP+100mM glucose+400 μ M AlCl₃ (e) MS+100mM glucose+1% sucrose (f) MS+RP as sole P source+100mM glucose+1% sucrose (g) MS+100mM glucose+1% sucrose+400 μ M AlCl₃ (h) MS+RP+100mM glucose+1% sucrose+400 μ M AlCl₃. C and T denote control and *Pseudomonas* P4 inoculated test. The arrow head pointing towards fluorescent green region indicates the overgrown *Pseudomonas* P4. The experimental procedures are as described in the text and the results are as monitored after 5-7 days of incubation.

Biochemical characterization

8.3.7: Effect of Pi levels on growth and media acidification profile of *Pseudomonas* P4 and *P. fluorescens* 13525

The specific growth rate of both *P. fluorescens* 13525 and *Pseudomonas* P4 improved with increase in the Pi levels, being the lowest on RP while the maximum on M9 minimal medium. However, *Pseudomonas* P4 had significantly higher growth rate as compared to *P. fluorescens* 13525 on all Pi levels (Table 8.5). *Pseudomonas* P4 acidified the extracellular medium irrespective of the Pi levels indicating efficient organic acid secretion. However, the time taken for media acidification gradually reduced from 96h on RP upto 27h on M9 minimal medium (Fig. 8.15; 8.16). Conversely, *P. fluorescens* 13525 could not acidify the medium on RP, 0.1mM and 1.0mM Pi while on 10mM Pi and M9 minimal medium media acidification was seen within 72h and 42h, respectively.

<i>Pseudomonas</i> strain	Specific growth rates on different Pi levels				
	RP	0.1mM	1.0mM	10mM	M9
<i>Pseudomonas</i> P4	0.041 ± 0.01	0.16 ± 0.017 **	0.24 ± 0.01 *	0.43 ± 0.06 **	1.09 ± 0.24 ***
<i>P. fluorescens</i> 13525	0.017 ± 0.05 β	0.089 ± 0.003 ***, γ	0.18 ± 0.03 *, γ	0.33 ± 0.04 **, β	0.44 ± 0.14 **, α

Table 8.5: Influence of Pi levels on specific growth rates of *Pseudomonas* P4 and *P. fluorescens* 13525. The specific growth rates have been calculated as described in text (Section 2.9.3) from log-phase cultures of both the *Pseudomonas* strains. The different Pi levels are as mentioned in the table while rest of the media composition was as described in Section 2.2.3 and 2.2.4. Experimental procedures are described in Section 2.9. The values are represented as Mean±S.E.M of 4-6 independent observations. * represents the comparison of the specific growth rates at two subsequent Pi levels for each strain. α, β and γ represent the comparison between the specific growth rates of *Pseudomonas* P4 and *P. fluorescens* 13525 at a particular Pi level. ***, α P<0.001; **, β P<0.01 and *, γ P<0.5

On the basis of these results, M9 minimal medium and Tris buffered minimal medium with RP (TRP) were used as P-sufficient and P-deficient conditions for studying the influence of Pi levels on the physiology and glucose catabolic pathways of *Pseudomonas* P4 and *P. fluorescens* 13525.

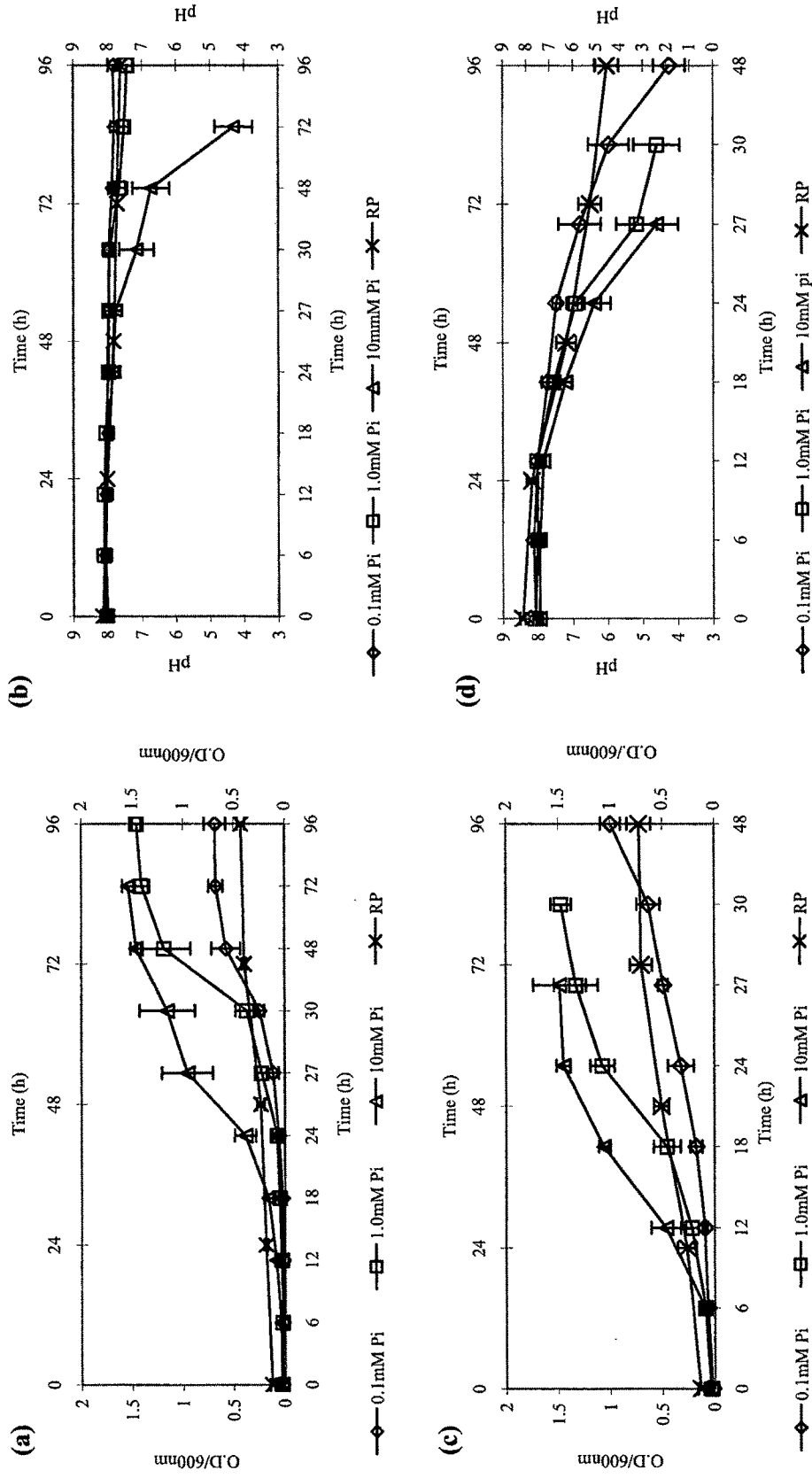


Fig. 8.15: Effect of Pi levels on growth and pH profile of *Pseudomonas* P4 and *P. fluorescens* 13525. The values O.D./600nm and pH are plotted as Mean \pm S.D of 6-8 independent observations (Section 2.9). (a)/(b) Growth and pH profile of *P. fluorescens* 13525 (c)/(d) Growth and pH profile of *Pseudomonas* P4 on different Pi levels.

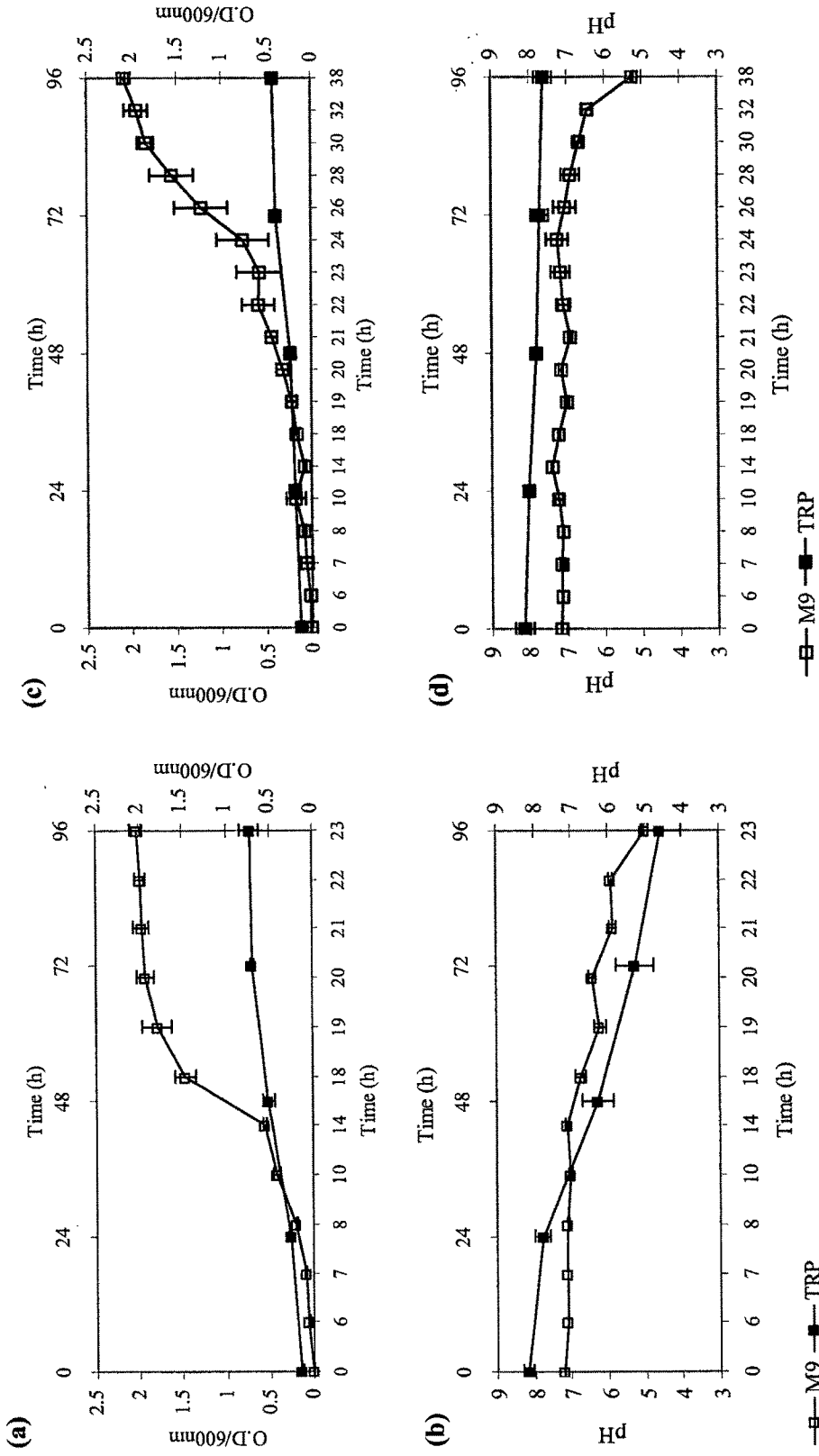


Fig. 8.16: Growth pattern and pH profile of *Pseudomonas P4* and *P. fluorescens 13525* under Pi-deficient and -sufficient conditions. O.D.₆₀₀ and pH values are plotted as Mean±S.D of 6-8 independent observations (Section 2.9). (a) / (b) Growth and pH profile of *Pseudomonas P4* on M9 and TRP medium, respectively (c) / (d) Growth and pH profile of *P. fluorescens 13525* on M9 and TRP medium, respectively.

8.3.8: Growth and glucose consumption profile of *Pseudomonas* P4 and *P. fluorescens* 13525 on TRP and M9 minimal media

Specific growth rates of both *Pseudomonas* P4 and *P. fluorescens* 13525 on TRP medium reduced by ~25 fold as compared to that on M9 medium (Table 8.6). Although, *Pseudomonas* P4 had ~6 fold lower glucose utilization rate on TRP medium, its total glucose utilization was ~1.3 fold higher than on M9 medium. On the contrary, glucose utilization rate and total glucose utilization of *P. fluorescens* 13525 reduced by ~2.8 and 6 fold, respectively on TRP medium as compared to M9 medium. Of the total glucose utilized by *Pseudomonas* P4 on M9 media, 77% was consumed by phosphorylative oxidation (as indicated by amount of glucose consumed) which was reduced to 49% on TRP medium; the remaining was utilized by direct periplasmic oxidation. On the other hand, in *P. fluorescens* 13525 on both TRP and M9 media, intracellular phosphorylative oxidation contributed to as high as 71% and 89% of total glucose utilization.

Comparing between the two strains, growth rate of *Pseudomonas* P4 was ~2 fold higher than *P. fluorescens* 13525 on both TRP and M9 minimal media (Table 8.6). Glucose utilization rates and total amount of glucose utilized by *Pseudomonas* P4 on TRP medium were ~2 and 12 fold higher than *P. fluorescens* 13525 while on M9 medium these parameters in *Pseudomonas* P4 were higher by ~4 and 1.5 fold higher.

Physiological parameters	<i>Pseudomonas</i> P4		<i>P. fluorescens</i> 13525	
	M9	TRP	M9	TRP
Sp. growth rate: k (hr^{-1})	1.09 ± 0.24	$0.04 \pm 0.01^{***}$	0.44 ± 0.14^a	$0.02 \pm 0.05^{***, a}$
Q_{Glc} (g/g/hr)	12.23 ± 5.37	$2.22 \pm 0.32^{***}$	3.04 ± 1.05^a	$1.11 \pm 0.19^{***, b}$
[#] Total glucose utilized (mM)	67.82 ± 7.06	$89.05 \pm 2.51^{**}$	46.39 ± 2.66^b	$7.56 \pm 1.01^{***, a}$
Glucose consumed (mM)	48.13 ± 4.12	$43.56 \pm 0.71^*$	41.14 ± 1.71^b	$5.80 \pm 0.58^{***, a}$

Table 8.6: Physiological parameters of *Pseudomonas* P4 and *P. fluorescens* 13525 on TRP and M9 minimal media. The specific growth rate (k) and specific glucose utilization rate (Q_{Glc}) were determined from mid log phase. [#] Total glucose utilized and glucose consumed were determined as described in Section 2.9.3. The values are derived from 5-7 independent observations. * denotes comparison of parameters of each strain on M9 and TRP medium while ^a ^b denote comparison between *Pseudomonas* P4 and *P. fluorescens* 13525 under a given media condition. ^{***}, ^a $P < 0.001$, ^{**}, ^b $P < 0.01$, * $P < 0.05$.

8.3.9: Organic acids secreted and enzyme activities in *Pseudomonas* P4 and *P. fluorescens* 13525 on TRP and M9 minimal media

Pseudomonas P4 secreted high amounts of gluconic acid on TRP medium unlike *P. fluorescens* 13525 which was unable to secrete significantly high levels of organic acids on TRP medium as also indicated by its inability to acidify the extracellular medium. However, gluconic acid levels and yield secreted by *Pseudomonas* P4 on M9 minimal medium respectively reduced by ~2.5 and 4.5 fold as compared to TRP medium (Table 8.7). On the other hand, *P. fluorescens* 13525 on TRP medium secreted ~2.9 fold lower gluconic acid levels, albeit its yield was ~10 times higher as compared to that on M9 medium. Additionally, on M9 medium both *Pseudomonas* P4 and *P. fluorescens* 13525 secreted pyruvic and acetic acids which were not detected on TRP medium. The variation in gluconic acid levels was accompanied by a concomitant ~1.7 fold higher GDH activity of *Pseudomonas* P4 on TRP medium as compared to M9 medium; while *P. fluorescens* 13525 had almost similar GDH activity on both the media (Fig. 8.17). G-6-PDH activities of *Pseudomonas* P4 and *P. fluorescens* 13525 on TRP medium were ~2 and 4 fold lower respectively, as compared to M9 medium. PYC activity in *Pseudomonas* P4 and *P. fluorescens* 13525 on TRP medium were lower by ~2 and ~4.7 fold respectively, than those determined on M9 medium. No significant PPC activity was detected in both *Pseudomonas* strains on any media condition.

Comparing the biochemical parameters between both the strains, gluconic acid secreted by *Pseudomonas* P4 was ~25 and 2 fold higher in levels and yield respectively than those secreted by *P. fluorescens* 13525 on TRP medium. Similarly, on M9 medium gluconic acid levels and yields secreted by *Pseudomonas* P4 were higher by ~3.8 and 3.5 folds respectively, as compared to *P. fluorescens* 13525. The levels and yield of pyruvic acid secreted by *Pseudomonas* P4 on M9 medium were ~3.5 and 2.6 fold higher respectively, as compared *P. fluorescens* 13525 while acetic acid levels secreted by both the strains were similar. In accordance with these differences in organic acid secretion, *Pseudomonas* P4 had ~5 fold higher GDH activity as compared to *P. fluorescens* 13525 on M9 medium which further increased by about 1.7 folds on TRP medium. On the other hand, G-6-PDH activity in *Pseudomonas* P4 was about ~1.9 fold higher than in *P. fluorescens* 13525 on TRP medium and remained similar on M9 medium. PYC activity in *Pseudomonas* P4 was ~4.8 and 2 folds lower than in *P. fluorescens* 13525 on M9 and TRP media respectively.

Organic acids		<i>Pseudomonas</i> P4		<i>P. fluorescens</i> 13525	
		M9	TRP	M9	TRP
Gluconic acid	Levels(mM)	19.69 ± 2.64 ^α	46.30 ± 4.73 ^{***, α}	5.25 ± 0.96	1.78 ± 0.48 ^{**}
	Yield	0.49 ± 0.07 ^α	2.14 ± 0.03 ^{***, α}	0.14 ± 0.04	1.46 ± 0.20 ^{***}
Pyruvic acid	Levels(mM)	11.37 ± 2.59 ^γ	UD	3.13 ± 0.44	UD
	Yield	0.13 ± 0.06 ^β	-	0.05 ± 0.01	-
Acetic acid	Levels(mM)	5.24 ± 1.39 ^{ns'}	UD	7.64 ± 1.77	UD
	Yield	0.04 ± 0.01 ^{ns'}	-	0.08 ± 0.02	-

Table 8.7: Organic acid secretion profile of *Pseudomonas* P4 and *P. fluorescens* 13525 on TRP and M9 minimal media. Results are expressed as Mean ± S.E.M of 4-8 independent observations. * denotes the comparison between the parameters for each strain on M9 and TRP minimal media conditions while ^α, ^β, ^γ, ^{ns'} denote the comparison between *Pseudomonas* P4 and *P. fluorescens* 13525 under a given media condition. The organic acids are estimated from late stationary phase cultures processed as described in the text (Section 2.9) and are expressed in terms of g/g glc⁻¹. dcw⁻¹. ^γ P<0.05, ^{***β} P<0.01, ^{***α} P<0.001, ^{ns'} non-significant.

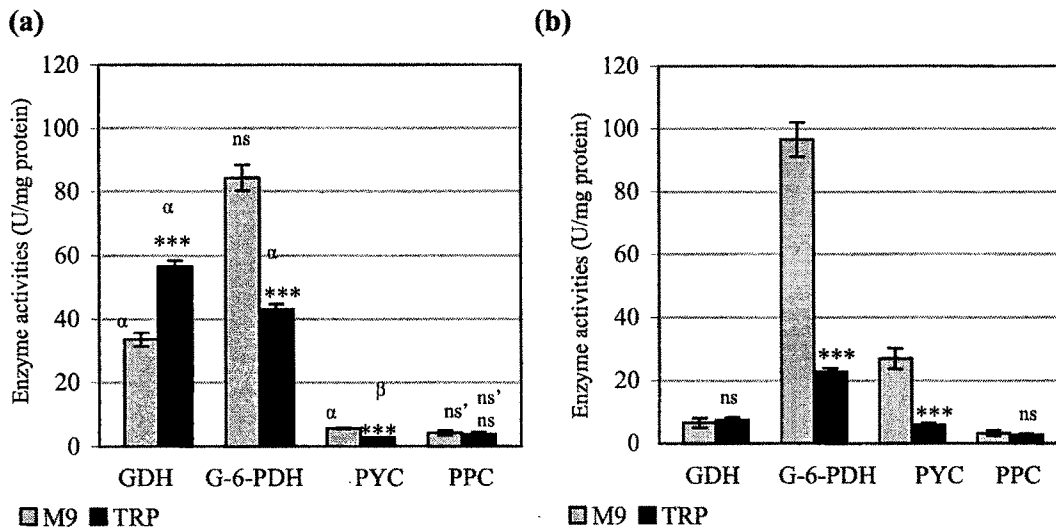


Fig. 8.17: Enzyme activities in *Pseudomonas* P4 and *P. fluorescens* 13525 on TRP and M9 minimal media (a) and (b) describes the enzyme activities estimated from mid-log to late log phase cultures of *Pseudomonas* P4 and *P. fluorescens* 13525 respectively, grown on M9 and TRP minimal media. The values are represented as Mean±S.E.M of 6-8 independent observations. *, ^{ns} denotes comparison of *P. fluorescens* 13525 and *Pseudomonas* P4 each on M9 and TRP media while ^α, ^{ns'} denote comparison between both strains on each medium. ^{***, α} P<0.0001; ^β P<0.009; ns, ^{ns'}=non-significant in both comparisons.

8.4: DISCUSSION

Numerous studies have dealt with isolating or developing efficient PSMs with additional PGPR activities (discussed in Chapter 1 and 7). Overexpression of *mps* genes like genes responsible for PQQ biosynthesis/transport in a variety of bacteria led to secretion of gluconic acids which could effectively solubilize Ca-P complexes (Rodriguez and Fraga, 1999). Genetic engineering could also improve nutrient utilizing ability leading to better survival of the inoculants (Khan et al., 2006). The present study dealt with an alternative strategy of integration of heterologous *S. elongatus ppc* gene which is important at anaplerotic node of central carbon metabolism in *Pseudomonas* like many other bacteria (Sauer and Eikmanns, 2005). *Pseudomonas* P4 was isolated by serendipity during pA172A plasmid integration experiments using soil isolates. The 16S rDNA sequencing identified *Pseudomonas* P4 as *Pseudomonas aeruginosa* spp. and was found to contain *ppc* plasmid in the genome. On account of its very efficient MPS ability, the biochemical and genetic basis of its MPS ability was investigated.

On account of 30% homology of *S. elongatus* PCC 6301 *ppc* gene with known *Pseudomonas ppc* genes, pA172A could have integrated by homologous recombination. Lack of homology between the genomic DNA fragment, obtained from plasmid recovery, and any of the known *ppc* sequences in the database suggested that probably homologous recombination was not the mechanism of pA172A genomic integration. Unusually, 95% identity with *E. coli* multi-drug efflux system also raised a possibility of homologous recombination at the tetracycline resistance gene of pA172A, since tetracycline resistance is mediated by an efflux pump (Schnappinger and Hillen, 1996; Chopra and Roberts, 2001). But there was no significant homology between tetracycline resistance gene as well as rest of pA172A backbone and the genomic DNA of the recovered plasmid, from which integration appeared to be an illegitimate recombination event. Since the site of integration did not coincide with any of the known glucose metabolism genes, there seems to be no direct correlation between the pA172A integration and gluconic acid mediated P-solubilization phenotype of *Pseudomonas* P4.

Pseudomonas P4 exhibited excellent MPS ability as demonstrated on PVK agar and TRP agar by secreting high amounts (~46mM) of gluconic acid. Gluconic acid has been the predominant organic acid found in many other gram-negative bacteria with

MPS ability (**Table 8.8**). *Pseudomonas* P4 is the most efficient pseudomonad whereas *Serratia marcescens* EB67 produced highest amount of gluconic acid of all. *E. asburiae* PSI3 has versatile MPS ability on a variety of sugars due to the broad substrate specificity of GDH enzyme (Gyaneshwar et al., 1999; Sharma et al., 2005). *Pseudomonas* P4 is unlike many other MPS bacteria which apparently are very efficient with respect to gluconic acid produced and Pi released, but are studied under unbuffered conditions which least mimic the actual soil buffering capacity which plays a crucial role in maintaining soluble Pi pool in the soil (Gyaneshwar et al., 1999; 2001). MPS pseudomonads are significant due to their plant growth promoting abilities. *Pseudomonas* P4 also secreted high levels of siderophore but no IAA production was observed (unpublished data). However, *Pseudomonas* P4 had adverse effect on the plant growth as it grew extensively on the root. Further experiments are required to determine whether *Pseudomonas* P4 has plant growth promotion or pathogenicity. *Pseudomonas aeruginosa* strains are known to belong to both these categories.

In addition to pseudomonads, *Rahnella aquatilis*, *Enterobacter asburiae* PSI3, *Erwinia* spp. and *Serratia* spp. producing high levels of gluconic acid, belong to *Enterobacteriaceae* family which primarily metabolize glucose via traditional EMP pathway. Contradictorily, in pseudomonads which also have emerged as potential MPS bacteria, periplasmic gluconic acid production is not only a mere P-solubilizing mechanism, but also constitutes a major glucose catabolism route and has supplementary role in P-solubilization. Hence, although highest gluconic acid producers belong to *Enterobacteriaceae* family as mentioned above, efficient MPS pseudomonads hold a distinct metabolic significance. The present study uniquely delineates the differences in the glucose catabolic pathways that underlie gluconic acid secretion in MPS pseudomonads.

Gluconic acid secretion is constitutive in most MPS bacteria including pseudomonads except being P-deficiency induced in *E. herbicola* (Goldstein and Liu., 1987) and *E. asburiae* PSI3 (Gyaneshwar et al., 1999). In addition to secreting high gluconic acid on TRP medium which is demonstrated to be P-limiting (Gyaneshwar et al., 1999), *Pseudomonas* P4 secreted gluconic acid even on M9 medium which is P-sufficient; albeit at lesser amount, (**Table 8.7**), indicating constitutive nature of GDH whose activities on both media correlate with the respective gluconic acid levels.

Microbial strain	Gluconic acid (mM)	Pi released (μ M)	Media specifications	Reference
<i>Pseudomonas</i> P4	46	437	100mM Tris buffered, 100mM glucose, RP, 96h	This study
<i>Pseudomonas cepacia</i> E37	20	86	1g% glucose, RP, 48h	Bar-Yosef et al., 1999
<i>Pseudomonas</i> sp. CDB35	27	522	100mM Tris buffered, 100mM (1.8g%) glucose, RP, 120h	Hameeda et al., 2006
<i>Burkholderia cepacia</i> CC-AI74	16.3	1470	TCP	Lin et al., 2006
<i>Azospirillum lipoferum</i> JA4	2 [#]	442	1g% glucose, 1g% fructose, TCP, 24h	Rodriguez et al., 2004
<i>Citrobacter</i> spp. DHRSS	19	520	50mM Tris buffered, 100mM (1.8g%) glucose, RP, 120h	Patel et al., 2008
<i>E. coli</i> HB101 + GAB1 gene of <i>P. cepacia</i> E37	3 (-PQQ) 32 (+PQQ)	nd	1g% glucose, TCP, 24h	Babu-khan et al., 1995
<i>Erwinia herbicola</i> EHO10	8.65 (i. a. units)	2571 [#]	1g% glucose+amino acids, TCP, 72h	Liu et al., 1992
<i>E. coli</i> HB101 + <i>mps</i> gene of <i>E. herbicola</i>	4.12 (i. a. units)	2204 [#]	1g% glucose+amino acids, TCP, 168h	Liu et al., 1992
<i>Enterobacter asburiae</i> PSI3	55	>800	100mM Tris buffered, 75mM (1.35g%) glucose, RP, 60h	Gyaneshwar et al., 1999; Sharma et al., 2005
<i>Rahnella aquatilis</i>	17.8	1691 [#]	1g% glucose, HAP, 72h	Kim et al., 1997
<i>E. coli</i> HB101 + <i>mps</i> gene of <i>Rahnella aquatilis</i>	46.8	>2941 [#]	1g% glucose, HAP, 72h	Kim et al., 1997; 1998
<i>Serratia marcescens</i> EB 67	67	1212	100mM Tris buffered, 100mM (1.8g%) glucose RP, 120h	Hameeda et al., 2006

Table 8.8: Gluconic acid production and Pi released from different mineral phosphates by certain efficient MPS bacteria. i. a. units-integrated area units, TCP-Tri calcium phosphate, PVK-Pikovaskya's medium, nq-not quantified. The medium is unbuffered unless and otherwise specified. [#] converted into comparable units. nd=not determined.

Glucose catabolism in pseudomonads occurs by two routes; GDH mediated extracellular direct oxidation pathway and intracellular phosphorylative pathway involving active glucose uptake followed by the action of glucokinase and G-6-PDH (Eisenberg et al, 1974; Lessie and Phibbs, 1984). The distribution of glucose between these two catabolic pathways would be responsible for MPS ability of pseudomonads. Higher glucose utilization rate and total amount of glucose utilized by *Pseudomonas* P4 on both P-limiting (TRP medium) and -sufficient (M9 medium) conditions and as compared to *P. fluorescens* 13525 (Table 8.6) were in agreement with higher growth rate and better organic acid secretion of *Pseudomonas* P4. On P-limiting condition, direct oxidation pathway predominantly catabolized more than half of the total glucose utilized, contrasting the P-sufficient condition in which phosphorylative oxidation predominated. Conversely, in *P. fluorescens* 13525 majority of the glucose was catabolized by phosphorylative pathway, on both P-limiting and sufficient conditions. Above observations were in accordance with higher GDH activity in *Pseudomonas* P4 which further increased upon P-limitation unlike in *P. fluorescens* 13525, thereby accounting for higher total glucose utilization and gluconic acid production by *Pseudomonas* P4 under P limitation than under P-sufficient condition. On the other hand, higher G-6-PDH activity (representing phosphorylative route) of *Pseudomonas* P4 under P limitation also correlated with its higher growth rate (Wolf et al., 1979) and glucose consumption as compared to *P. fluorescens* 13525 which consumed very less amount of glucose concomitant with its lower growth rate. However, under P sufficiency, G-6-PDH activity in both *Pseudomonas* strains was similar despite significantly differing growth rates.

On P-limiting condition, *Pseudomonas* P4 and *P. fluorescens* 13525 secreted only gluconic acid, which also suggested that direct oxidation pathway was predominant. These strains secreted pyruvic and acetic acids in addition to gluconic acid on P-sufficient condition which indicated the increased contribution of phosphorylative pathway, since metabolite like acetic acid has been implicated in aerobic carbon overflow metabolism in *E. coli* (Farmer and Liao, 1997). However, low levels of acetic acid in pseudomonads could be attributed to the efficient TCA cycle (Fuhrer et al., 2005). On the other hand, variations in pyruvic acid could be due the unusual pyruvate shunt regulated by PYC activity. High pyruvate secretion in *Pseudomonas* P4 under P-sufficient condition could be due to lower PYC activity which might be responsible for pyruvate accumulation. This was supported by high PYC activity in *P. fluorescens*

13525 which secreted low levels of pyruvate. Importance of PYC in glucose assimilation in pseudomonads, especially in absence of PPC is evident from the inability of *P. aeruginosa* PAO *pyc*⁻ to utilize C₆ compounds as source of carbon and energy (Phibbs et al., 1974). Under P-limitation, reduction in ATP utilizing PYC activity in both *Pseudomonas* strains coupled with absence of acetic and pyruvic acid secretion implicated compromised central metabolism. Both *Pseudomonas* strains had negligible PPC activity suggesting that PYC solely contributed towards OAA formation.

Our results demonstrate that P levels apparently influence the glucose distribution between the two catabolic pathways. *P. aeruginosa* in presence of glucose and nitrate under anaerobic conditions lacked direct oxidation pathway which increased with oxygen availability (Lessie and Phibbs, 1984). Similarly, in *P. aeruginosa* PAO1 and *P. fluorescens* under glucose limitation, catabolism primarily occurred through phosphorylative route while in glucose excess direct oxidation route was preferred (Lessie and Phibbs, 1984). In *P. fluorescens* E20 glucose catabolism shifted from direct oxidation to phosphorylative route with increase in temperature (Lessie and Phibbs, 1984). *P. cepacia* catabolized non-glucose carbon sources by phosphorylative pathway. Hence, glucose and oxygen availability are known to influence the operation of these two catabolic pathways. However, so far, no studies reported the effect of P status on glucose distribution between these two pathways in pseudomonads.

Under P-limitation, due to compromised metabolic status, intracellular phosphorylative pathway of glucose oxidation in both the pseudomonads was subdued while enhanced direct oxidative pathway was preferred probably as it could benefit the metabolic status since GDH activity is directly coupled to electron transfer and generation of proton motive force (van Schie et al, 1985). This also could probably explain why most of the rhizospheric MPS bacteria employ direct oxidation pathway mediated gluconic or 2-ketogluconic acid secretion for P-solubilization. Compromised overall metabolic status of *P. fluorescens* 13525 under P-deficient conditions was overcome in *Pseudomonas* P4 by its ability to shift the metabolism towards direct oxidation pathway producing high gluconic acid levels which facilitated ATP generation by improving Pi availability. Present study explains the metabolic flexibility/rigidity behind gluconic acid secretion in P-solubilizing pseudomonads which could facilitate metabolic engineering strategies for enhancing the MPS ability of *Pseudomonas* strains.